Making a case for full-polarimetric radar remote sensing

Jeremy Nicoll

Alaska Satellite Facility, University of Alaska Fairbanks

Polarization States of a Coherent Plane Wave

electric field vector

vertically polarized

horizontally polarized

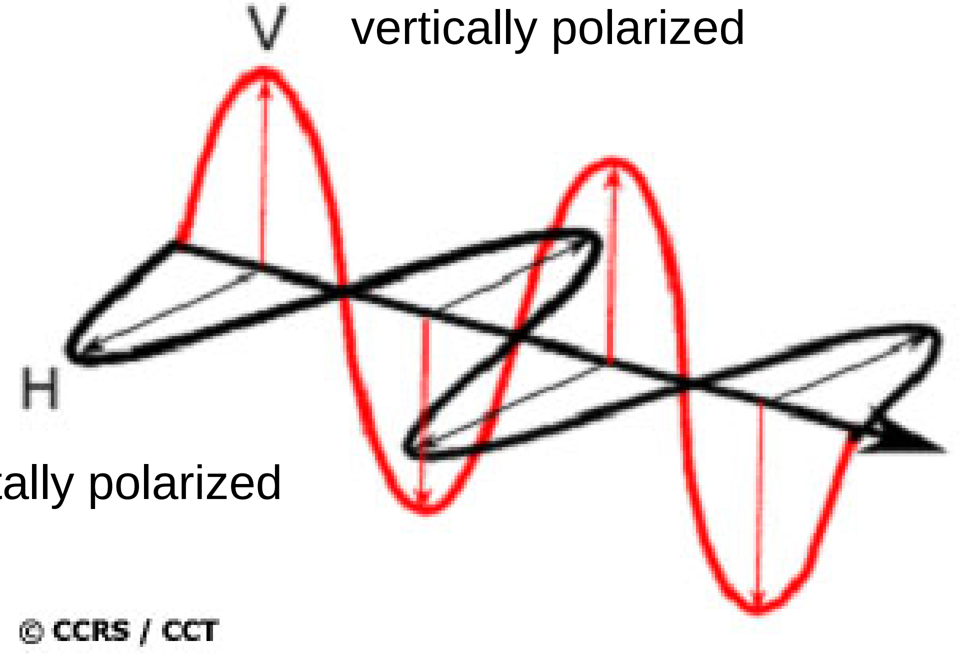

Polarimetric SAR System Configurations

- **single pol:**
  - VV or HH (or possibly HV or VH)
- **dual pol:**
  - HH and HV, VV and VH, or HH and VV
- **quad pol (fully polarimetric):**
  - HH, VV, HV, and VH
- **Polarization types**
  - **Linearly polarized**
  - **Circularly polarized**
  - **Elliptically polarized**

relative phase between channels is important information

Polarimetric SAR Measurement

HH: H transmit, H receive
VV: V transmit, V receive
HV: H transmit, V receive
VH: V transmit, H receive

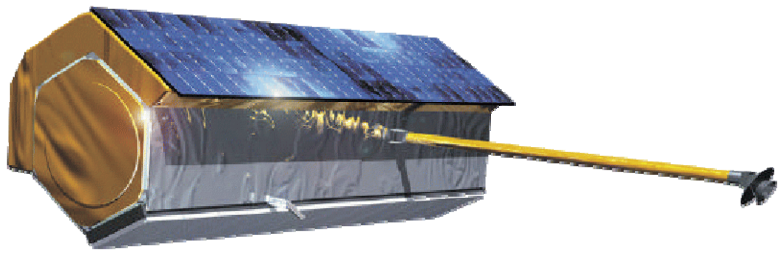

receive: **H** and / or **V**

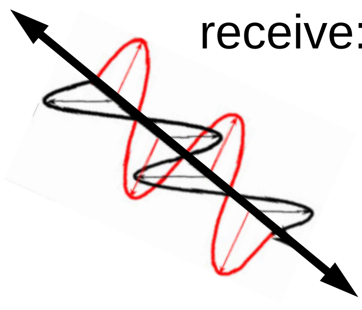

transmit: **H** and / or **V**

Penetration of Microwaves

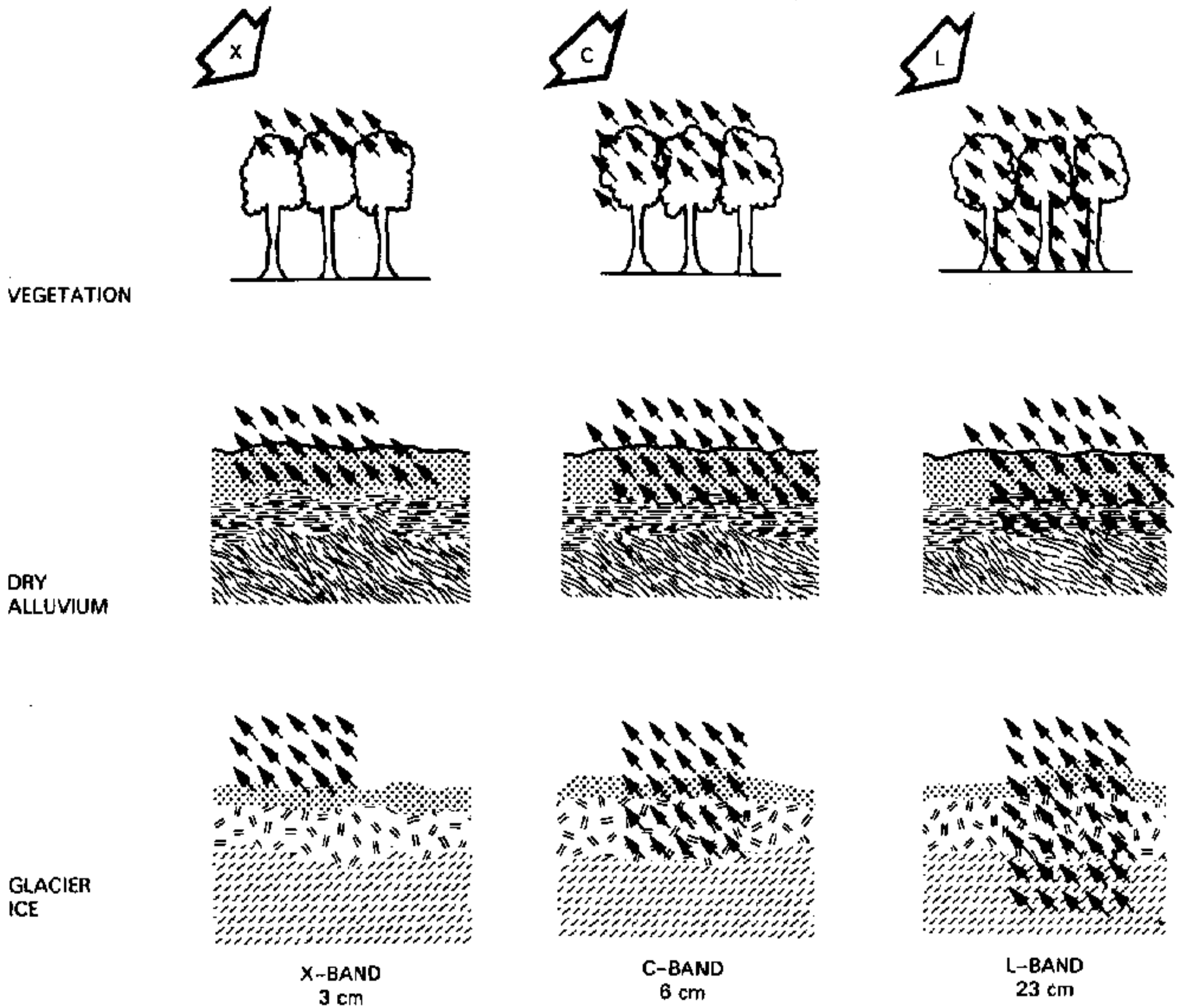

from: FAO - Radar imagery: theory and interpretation, lecture notes

Multi-Polarization SAR Image (SIR-C 1994)

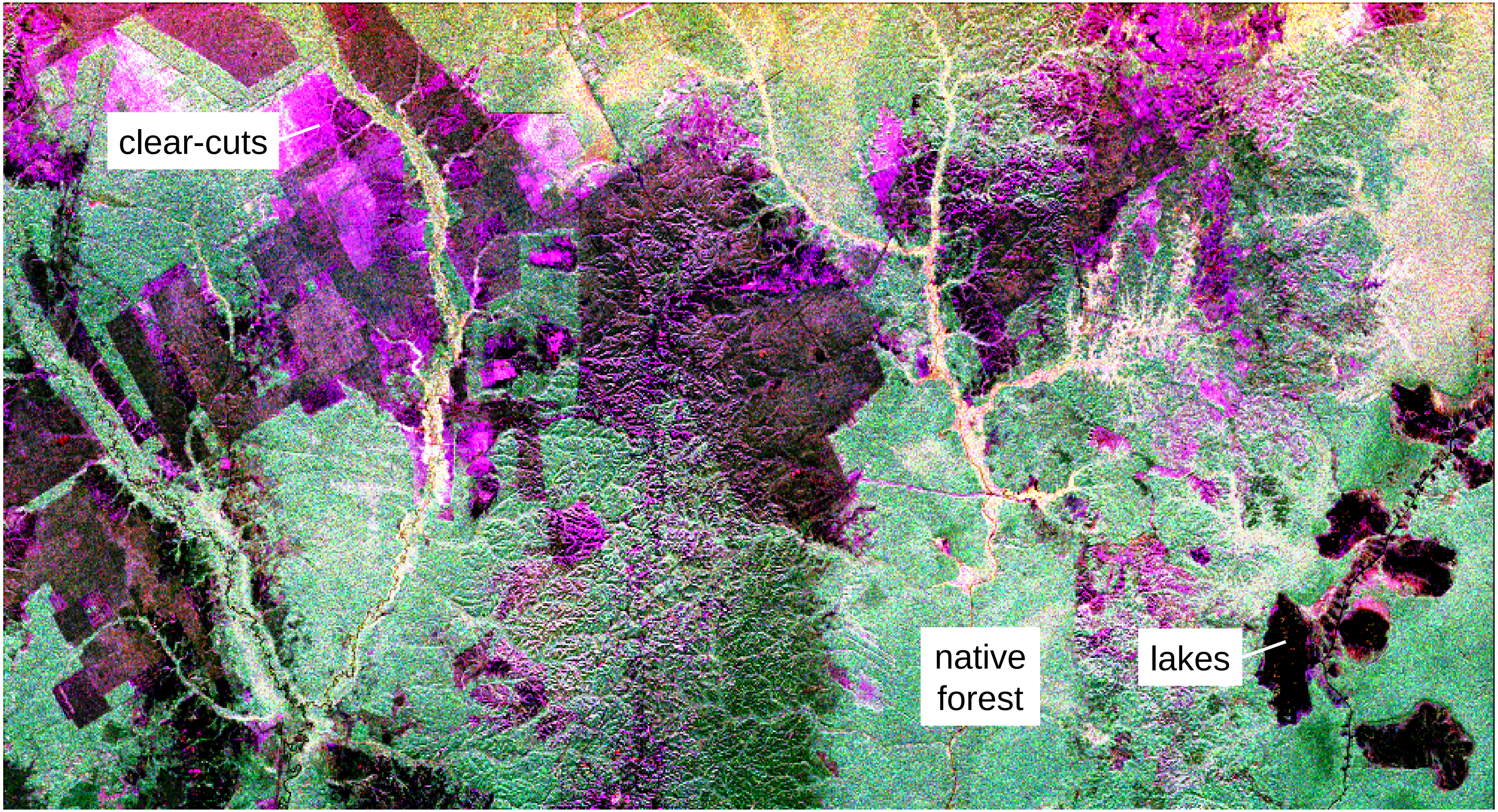

red = L-HH green = L-HV blue = L-VV courtesy of JPL

Central Sumatra, Indonesia (50 km x 100 km)

Multi-Polarization/Multi-Frequency SAR Image (SIR-C/X-SAR 1994)

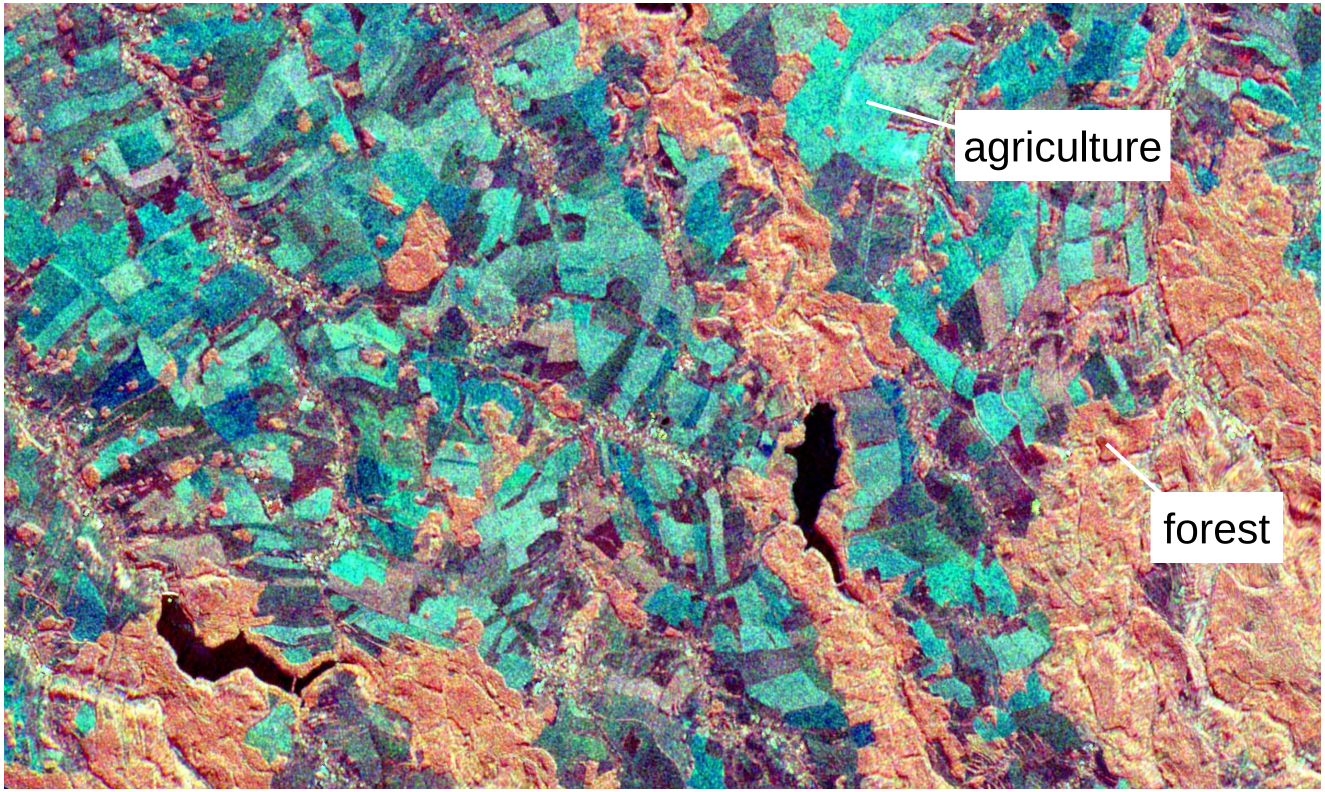

red = L-HV green = C-TP blue = X-VV

Freital, Saxonia, Germany (11 km x 20 km)

Representation of the data – Jones Matrix

- Send out a polarized wave (vertical, horizontal, or some combination).
- The wave interacts with a scatterer, causing a linear transformation of the wave.
- The wave is detected.
- S can be reduced to the independent parameters.

$$\vec{E}^{tr} = E_h^{tr}\vec{e}_h + E_v^{tr}\vec{e}_v$$

$$\vec{E}^{re} = [S]\,\vec{E}^{tr} = \begin{bmatrix} E_h^{re} \\ E_v^{re} \end{bmatrix} = \frac{e^{ik_0 r}}{r} \begin{bmatrix} S_{hh} & S_{hv} \\ S_{vh} & S_{vv} \end{bmatrix} \begin{bmatrix} E_h^{tr} \\ E_v^{tr} \end{bmatrix}$$

$$[S] = e^{i\phi_0} \begin{bmatrix} |S_{hh}| & |S_x|e^{i(\phi_x - \phi_0)} \\ |S_x|e^{i(\phi_x - \phi_0)} & |S_{vv}|e^{i(\phi_{vv} - \phi_0)} \end{bmatrix}$$

Equations from SAR Polarimetry Tutorial by Martin Hellmann

Representation of the data – Coherency matrix

- But my resolution cell is larger than my scatterers …
- I can have more than one scatterer, and more than one type of scatterer in my resolution cell …

$$[S] = \begin{bmatrix} S_{11} & S_x \\ S_x & S_{22} \end{bmatrix} \Rightarrow \vec{k} = \vec{k}_P = \begin{bmatrix} S_{11} + S_{22} \\ S_{11} - S_{22} \\ 2S_x \end{bmatrix}$$

  – Convert Jones to a Pauli matrix

$$[T]_{3\times3} = \left\langle \vec{k}_{P3}\vec{k}_{P3}^{\dagger} \right\rangle = \frac{1}{2}\begin{bmatrix} \langle|A|^2\rangle & \langle AB^*\rangle & \langle AC^*\rangle \\ \langle A^*B\rangle & \langle|B|^2\rangle & \langle BC^*\rangle \\ \langle A^*C\rangle & \langle B^*C\rangle & \langle|C|^2\rangle \end{bmatrix} \; where \begin{cases} A = S_{hh} + S_{vv} \\ B = S_{hh} - S_{vv} \\ C = 2S_x \end{cases}$$

  – Create a coherency matrix (<XY> denote ensemble averaging, assuming homogeneity.

Equations from SAR Polarimetry Tutorial by Martin Hellmann

Decomposition of the data

- Goal – separate contributions into different scattering mechanisms.

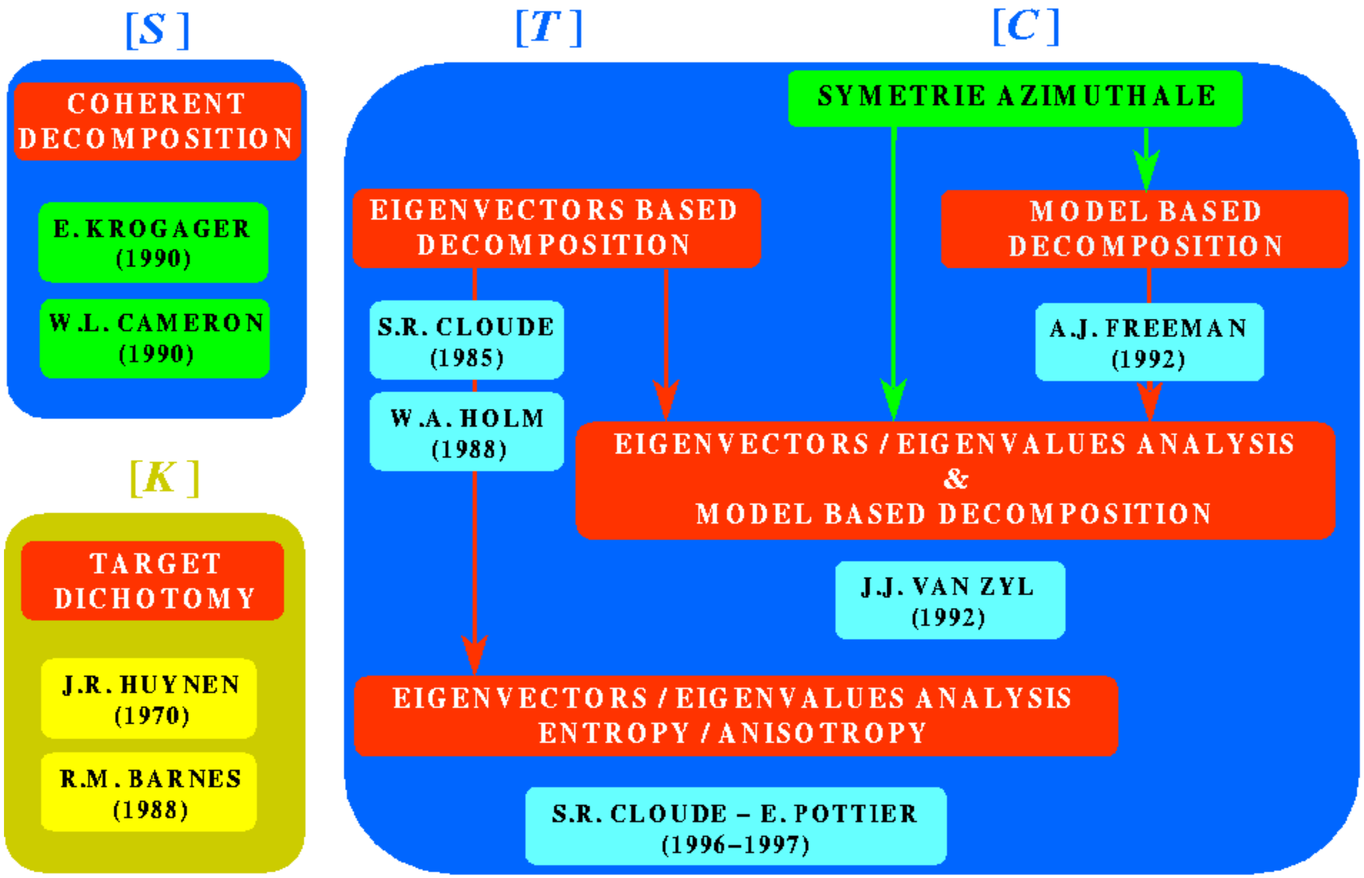

Overview of Decomposition theorems (from Eric Pottier)

Pauli Decomposition

•

Pauli matrix	*scattering type*	*interpretation*
$\begin{bmatrix} 1 & 0 \\ 0 & 1 \end{bmatrix}$	odd–bounce	surface, sphere, cornerreflectors
$\begin{bmatrix} 1 & 0 \\ 0 & -1 \end{bmatrix}$	even–bounce	dihedral
$\begin{bmatrix} 0 & 1 \\ 1 & 0 \end{bmatrix}$	even–bounce $\pi/4$ tilted	$\pi/4$ tilted dihedral
$\begin{bmatrix} 0 & -i \\ i & 0 \end{bmatrix}$	cross–polariser	not existent for backscattering

Image from E-SAR over Oberpfaffenhofen (from SAR Polarimetry Tutorial by Martin Hellmann)

The Cloude Decomposition

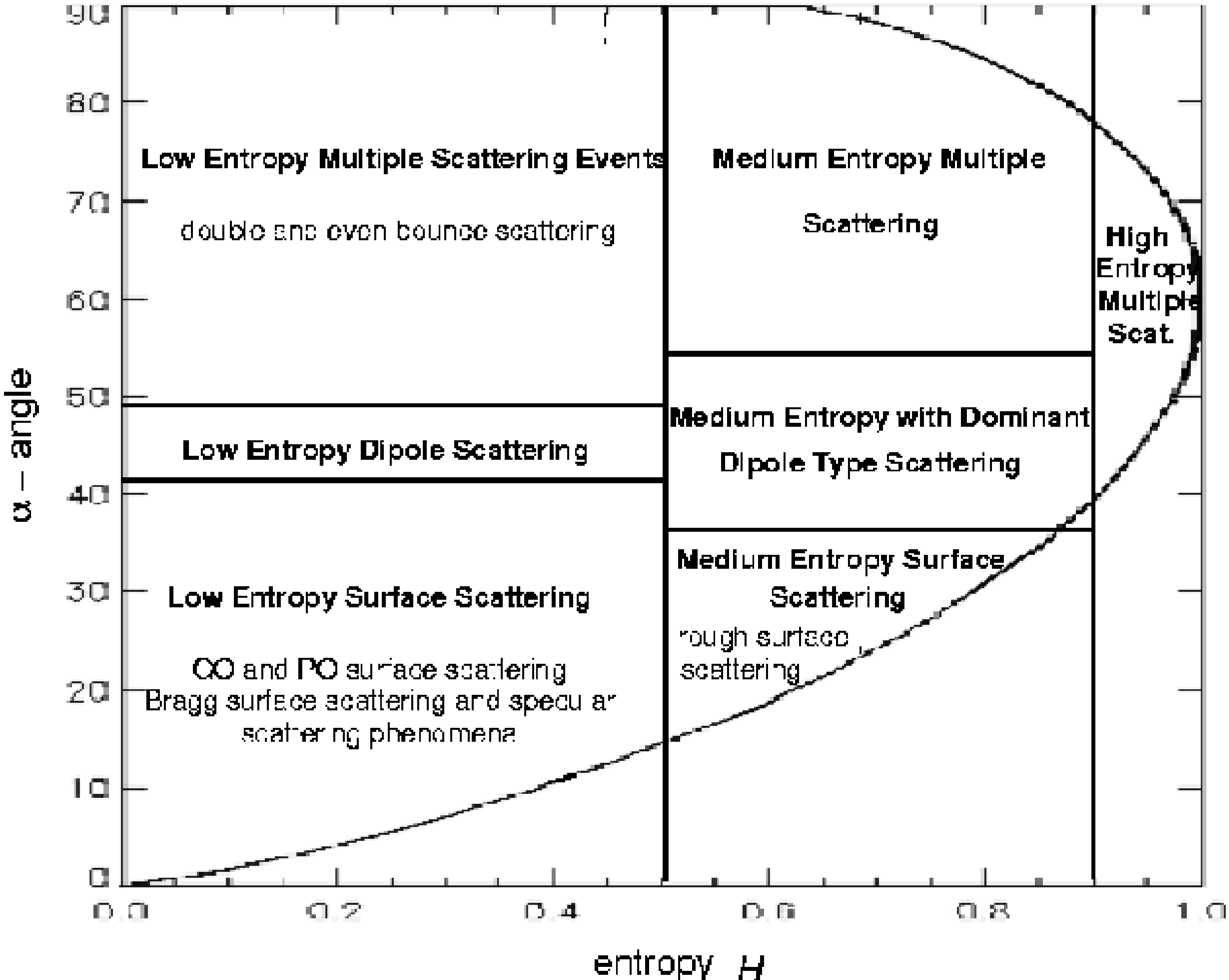

Entropy, Anisotropy

- **Perform Eigenvalue decomposition of coherency matrix into orthogonal scattering mechanisms.**
  - **Each "decomposed" matrix represents a single scattering mechanism.**

$$[T] = \sum_{n=1}^{3} \lambda_n [T_n] = \lambda_1(\vec{e}_1 \cdot \vec{e}_1^{\dagger}) + \lambda_2(\vec{e}_2 \cdot \vec{e}_2^{\dagger}) + \lambda_3(\vec{e}_3 \cdot \vec{e}_3^{\dagger})$$

- **Compare eigenvalues**
  - **If they are nearly the same, there is no dominant scattering mechanism. Entropy =>1.**
  - **If one dominates, Entropy=>0.**

- **Anisotropy**
  - **Compare second and third eigenvalues. The more they are different, the larger the anisotrpoy. A high anisotropy says the second eigenvalue dominates, while a low anisotropy says the 2nd and 3rd are equally important.**

Average Scattering mechanism (alpha)

- Any Pauli vector (and therefore Jones matrix) can be rotated to become the unity vector.

$$\begin{bmatrix} 1 \\ 0 \\ 0 \end{bmatrix} = \begin{bmatrix} cos\alpha & sin\alpha & 0 \\ -sin\alpha & cos\alpha & 0 \\ 0 & 0 & 1 \end{bmatrix} \begin{bmatrix} 1 & 0 & 0 \\ 0 & cos\beta & sin\beta \\ 0 & sin\beta & cos\beta \end{bmatrix} \begin{bmatrix} e^{i\phi} & 0 & 0 \\ 0 & e^{i\delta} & 0 \\ 0 & 0 & e^{i\gamma} \end{bmatrix} \vec{k}$$

- Alpha is the first rotation term. Its interpretation is:

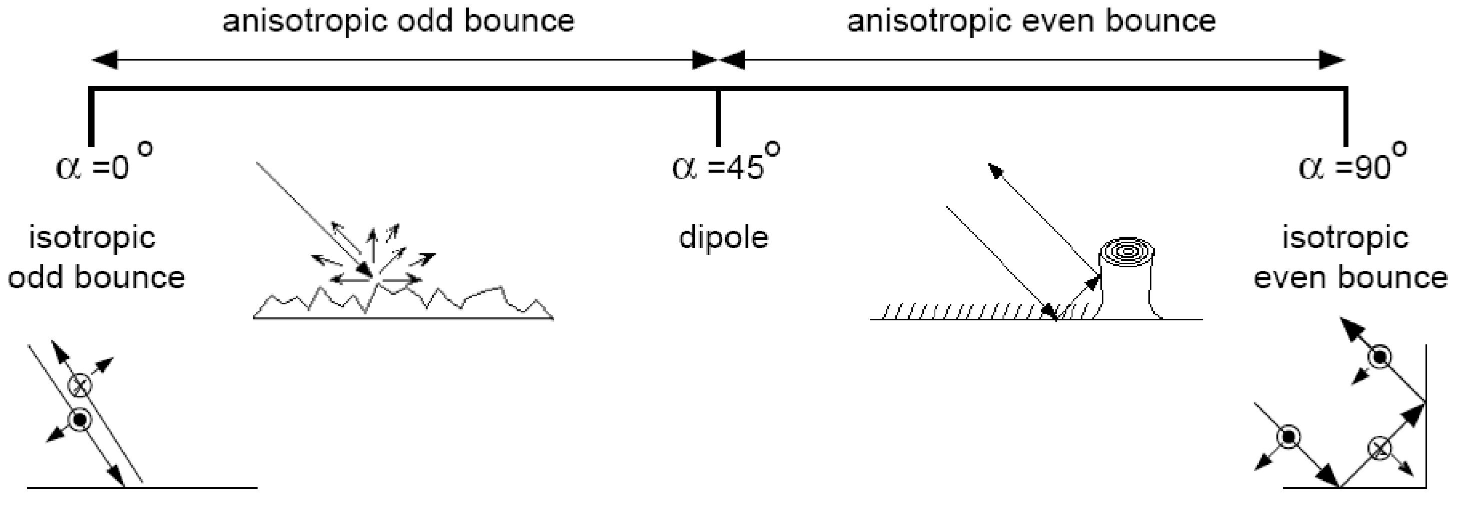

- Other terms are target orientation and phase angles.

H-alpha plane

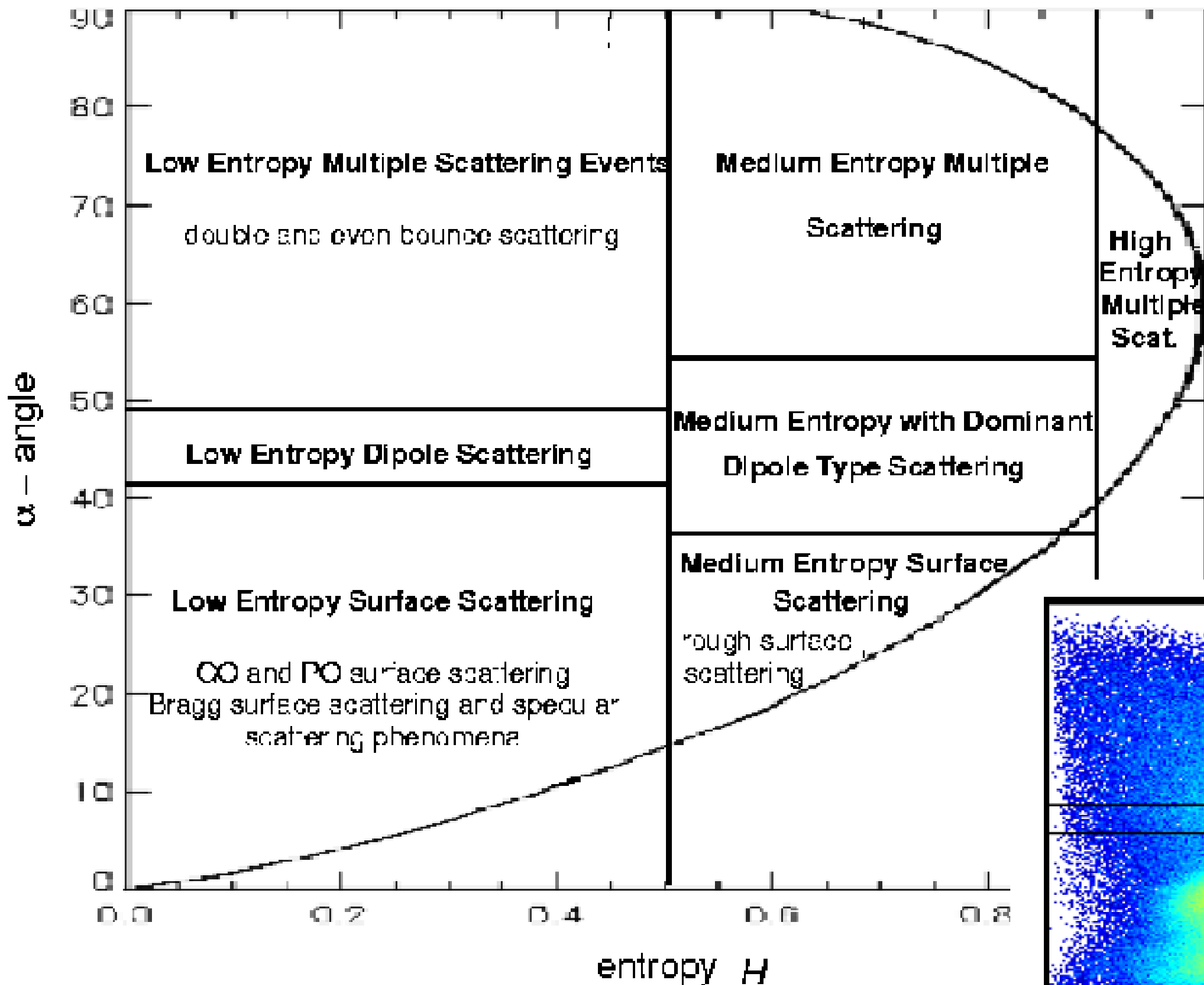

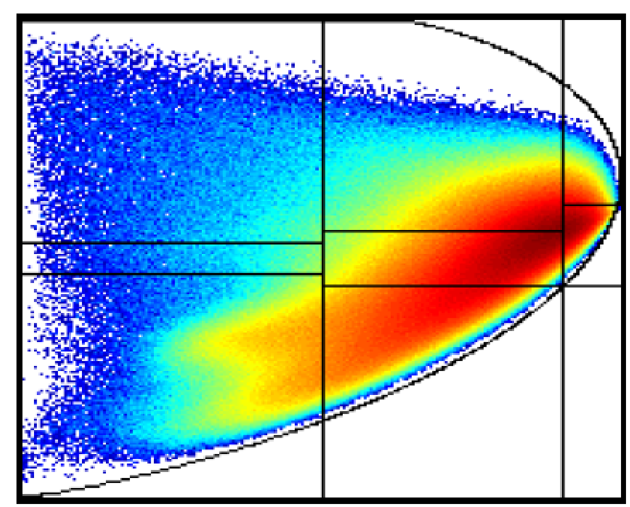

HA-alpha imagery

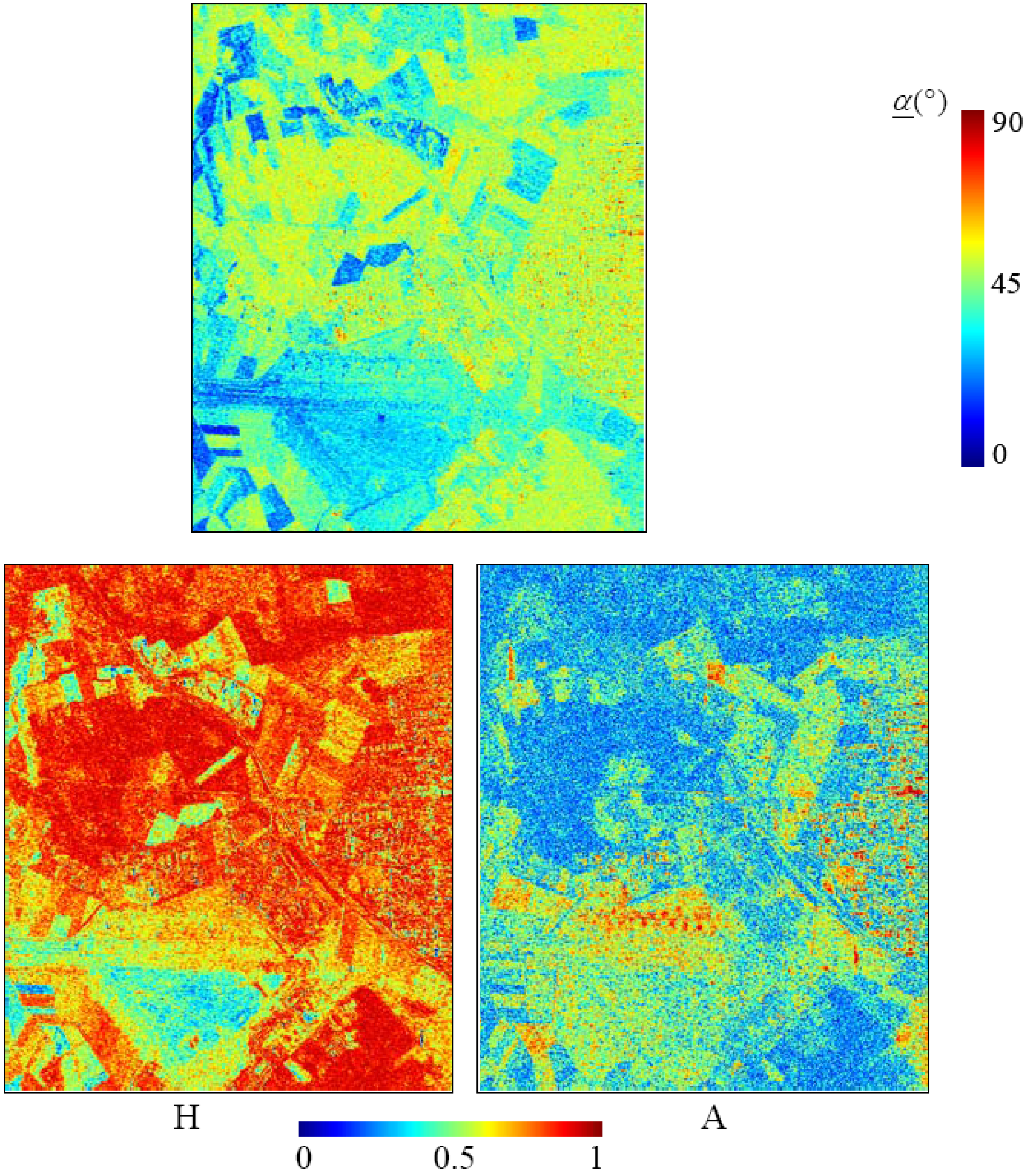

- **From ESA POLSARPRO manual, chapter 5.**

Applications

- Surface roughness
- Surface slopes
- Soil moisture
- Vegetation biomass
- Vegetation heights
- Tree species
- Snow monitoring
- Water equivalent ice thickness
- Meteorology
- Hydrology
- Geology
- Topography
- Cartography
- De-mining
- Sea ice
- Oceanography
- Forestry
- Crop classification

Crops

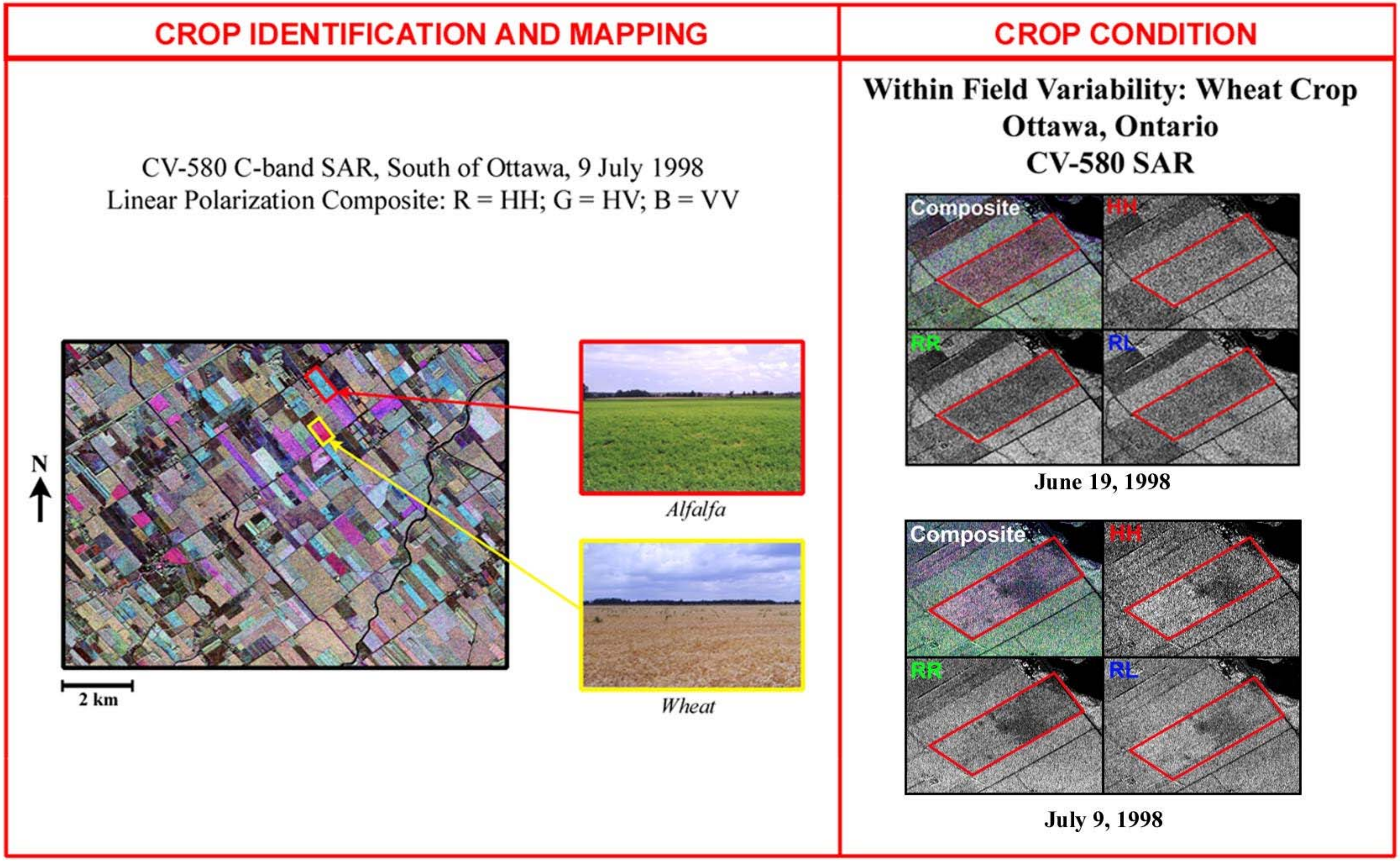

Image courtesy of Canadian Centre for Remote Sensing

Sea Ice

- Possible to better distinguish ice edge from windswept ocean
- Better ice type classification than single pol.

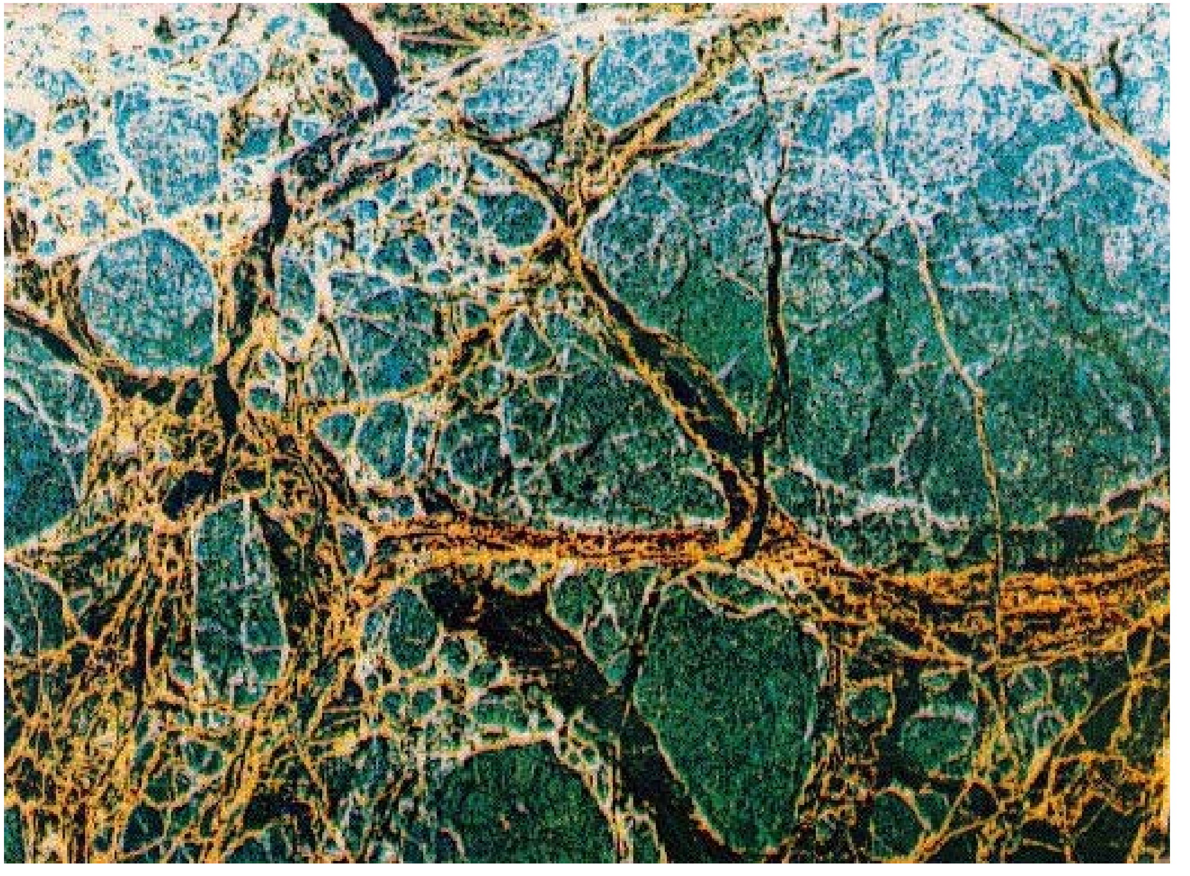

- Image by JPL's AIRSAR from S. V. Nghiem and C. Bertoia, "Multi-Polarization C-Band SAR Signatures of Arctic Sea Ice," IGARSS 2001.

- " … the polarimetric parameters include a significant amount of soil moisture and surface roughness information."
- C. Thiel, S. Gruenler, M. Herold, V. Hochschild, G. Jaeger & M. Hellmann Interpretation and Analysis of Polarimetric L-Band E-SAR-Data for the Derivation of Hydrologic Land Surface Parameters, IGARSS 2001

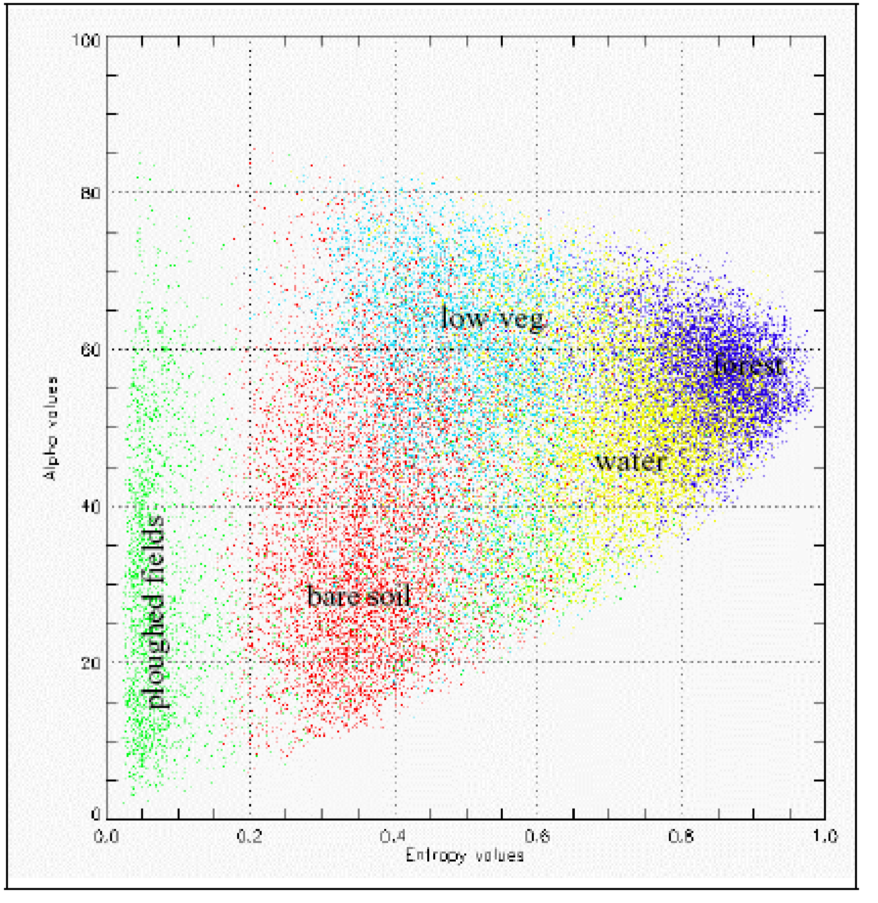

PolInSAR

- "SAR interferometry is today an established technique for estimation of the height location of scatterers through the phase difference in images acquired from spatially separated apertures at either end of a baseline … scattering polarimetry is sensitive to the shape, orientation, and dielectric properties of scatterers … In polarimetric SAR interferometry (Pol-InSAR), both techniques are coherently combined to provide sensitivity to the vertical distribution of different scattering mechanisms. Hence, it becomes possible to investigate the 3D structure of volume scatterers such as vegetation and ice, promising a breakthrough in radar remote sensing problems."
- Krieger, Papathanassiou, Cloude, "Spaceborne Polarimetric SAR Interferometry: Performance Analysis and Mission Concepts" -- EURASIP Journal on Applied Signal Processing 2005:20, 3272–3292

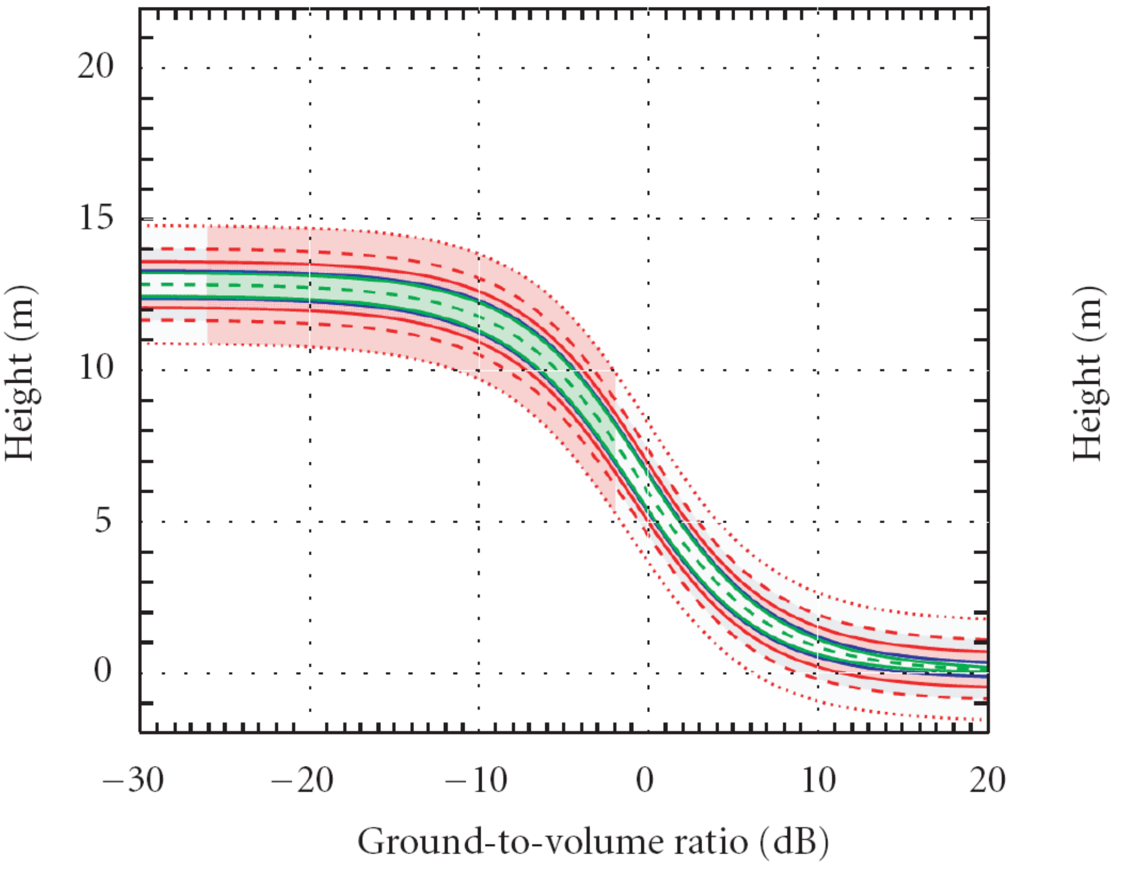

Forest Biomass

- Biomass determined from tree height, as a direct result of POLINSAR. Some dependence on tree type in the model.

- T. Mette, K. Papathanassiou, I. Hajnsek, “Biomass estimation from polarimetric SAR interferometry over heterogeneous forest terrain,” IGARSS 2004

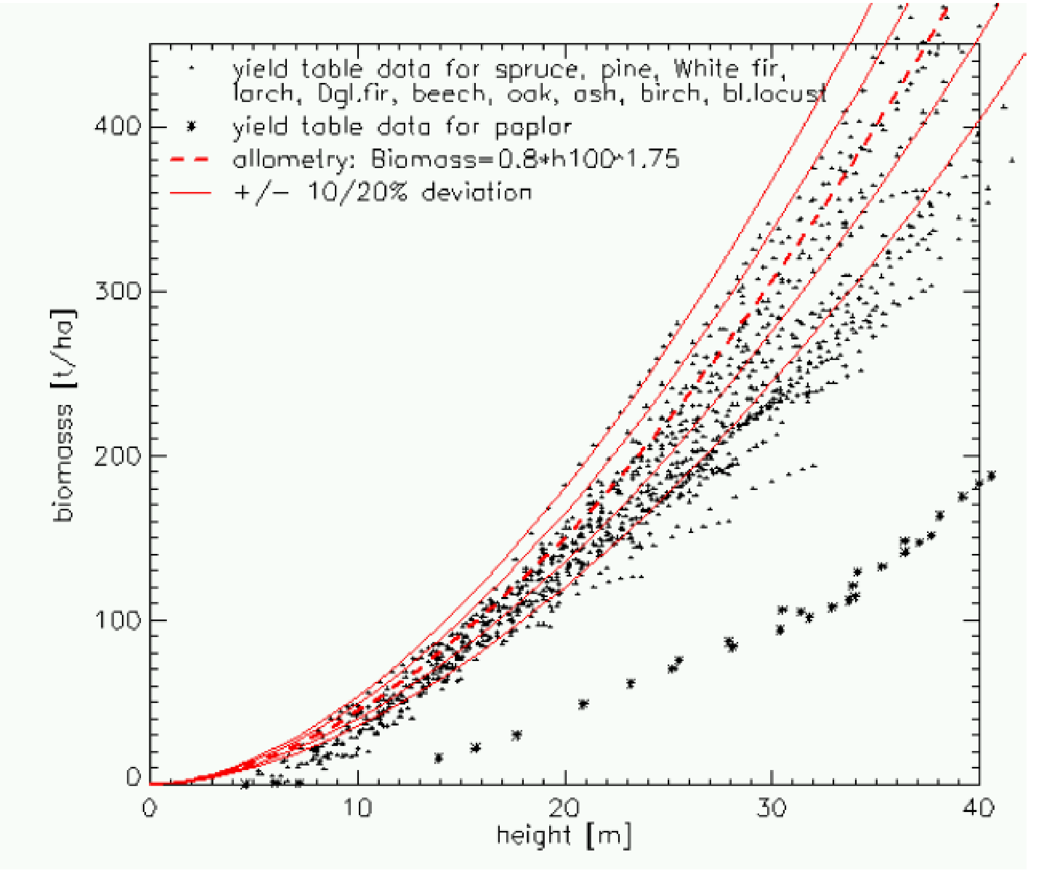

Advanced Polarimetric Instruments

- Multifrequency
- Multi-instrument
- Sparse matrix / Circular polarized / Linear-circular

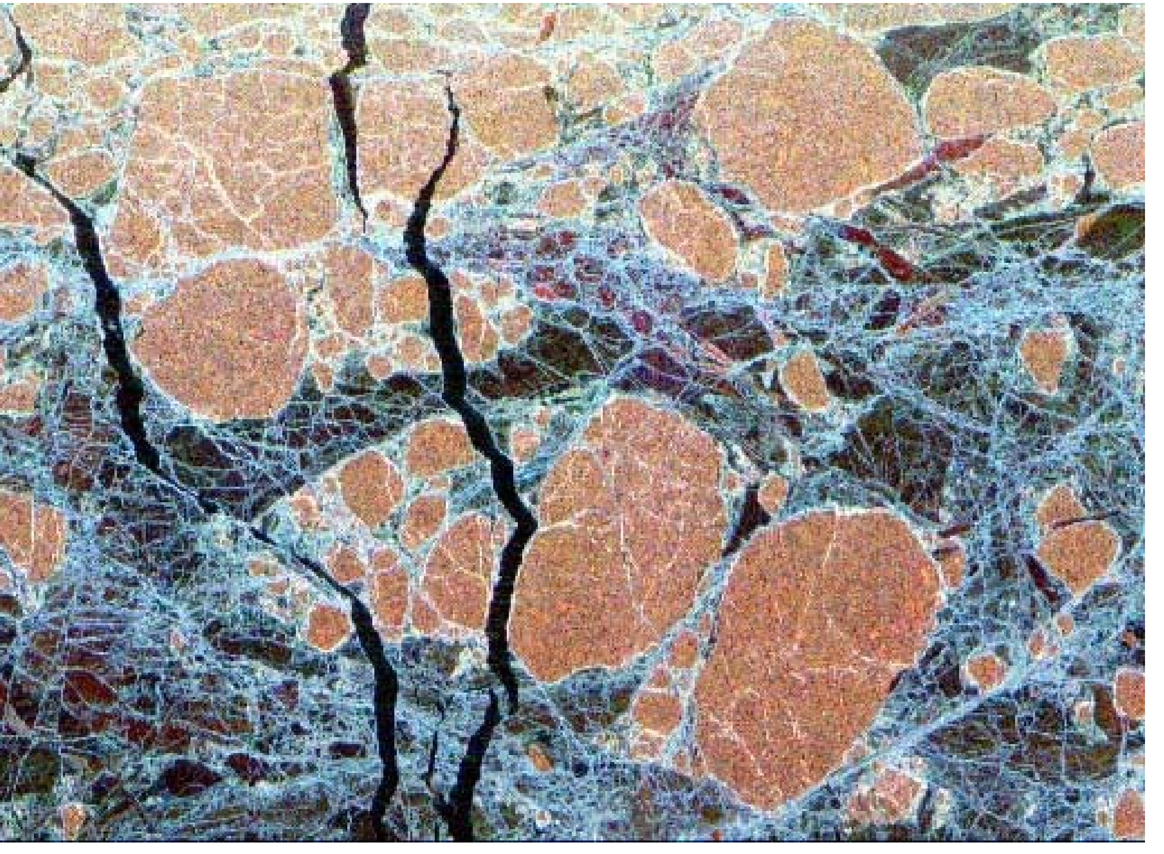

RGB image using the total power (in dB) of the three frequencies (red=C-band, green=L band, blue=P-band.) from B. Scheuchl, I. Hajnsek, and I. Cumming, "**Sea Ice Classification Using Multi-Frequency Polarimetric SAR Data," IGARSS 2002**

Calibration

- Channel imbalance (f)
- Cross-talk (delta)
- Noise (N)
- Faraday rotation (omega)

$$\begin{pmatrix} M_{\mathrm{hh}} & M_{\mathrm{vh}} \\ M_{\mathrm{hv}} & M_{\mathrm{vv}} \end{pmatrix} = \mathrm{A}(\mathrm{r},\theta)e^{\mathrm{j}\phi} \begin{pmatrix} 1 & \delta_2 \\ \delta_1 & 1 \end{pmatrix} \begin{pmatrix} 1 & 0 \\ 0 & f_1 \end{pmatrix}$$
$$\cdot \begin{pmatrix} \cos\Omega & \sin\Omega \\ -\sin\Omega & \cos\Omega \end{pmatrix} \begin{pmatrix} S_{\mathrm{hh}} & S_{\mathrm{vh}} \\ S_{\mathrm{hv}} & S_{\mathrm{vv}} \end{pmatrix}$$
$$\cdot \begin{pmatrix} \cos\Omega & \sin\Omega \\ -\sin\Omega & \cos\Omega \end{pmatrix} \begin{pmatrix} 1 & 0 \\ 0 & f_2 \end{pmatrix}$$
$$\cdot \begin{pmatrix} 1 & \delta_3 \\ \delta_4 & 1 \end{pmatrix} + \begin{pmatrix} N_{\mathrm{hh}} & N_{\mathrm{vh}} \\ N_{\mathrm{hv}} & N_{\mathrm{vv}} \end{pmatrix}$$

Ionospheric Effects on Broadband Linearly Polarized SAR Signals

- phase delay:

$$\tau_{ph} = -\frac{\phi(f_0)}{2\pi f_0} \approx -\frac{2 \cdot 40.28}{c f_0^2} TEC$$

→ **Advance of SAR phase**

- group delay:

$$\tau_{gr} = -\frac{1}{2\pi}\frac{d\phi(f)}{df}\bigg|_{f=f_0} \approx \frac{2 \cdot 40.28}{c f_0^2} TEC$$

→ **Delay of signal envelope**

- Non-linear residual phase within SAR bandwidth

$$\delta\phi_r(f)$$

→ **Range blurring of SAR image**

- Faraday Rotation

$$\Omega = \frac{K}{f^2}\int NH \cos\theta \sec\chi \, dh$$

→ **Change of scattering matrix**

FR Estimation from imagery

- Measured Scattering matrix of a sufficiently calibrated SAR system

$$\begin{bmatrix} M_{hh} & M_{vh} \\ M_{hv} & M_{vv} \end{bmatrix} = \begin{bmatrix} \cos\Omega & \sin\Omega \\ -\sin\Omega & \cos\Omega \end{bmatrix} \cdot \begin{bmatrix} S_{hh} & S_{vh} \\ S_{hv} & S_{vv} \end{bmatrix} \cdot \begin{bmatrix} \cos\Omega & \sin\Omega \\ -\sin\Omega & \cos\Omega \end{bmatrix}$$

- Direct estimation from scattering matrix (Freeman, 2004):

$$\Omega = \frac{1}{2}\tan^{-1}\left[\frac{\left(M_{vh} - M_{hv}\right)}{\left(M_{vv} + M_{vv}\right)}\right]$$

- Estimation from circular basis (Bickel & Bates, 1965):

$$\begin{bmatrix} Z_{11} & Z_{12} \\ Z_{21} & M_{22} \end{bmatrix} = \begin{bmatrix} 1 & j \\ j & 1 \end{bmatrix} \cdot \begin{bmatrix} M_{hh} & M_{vh} \\ M_{hv} & M_{vv} \end{bmatrix} \cdot \begin{bmatrix} 1 & j \\ j & 1 \end{bmatrix}$$

$$\Omega = \frac{1}{4}\arg\left(Z_{12}Z_{21}^{*}\right)$$

FR Estimation Toolbox

- Full-pol PalSAR data
- 10x10 averaging of the complex valued SAR data for noise reduction
- FR estimation according to Bickel & Bates method
- Statistics as well as range and azimuth analysis
- FR angles of up to 4.5º found

PalSAR data over Washington DC

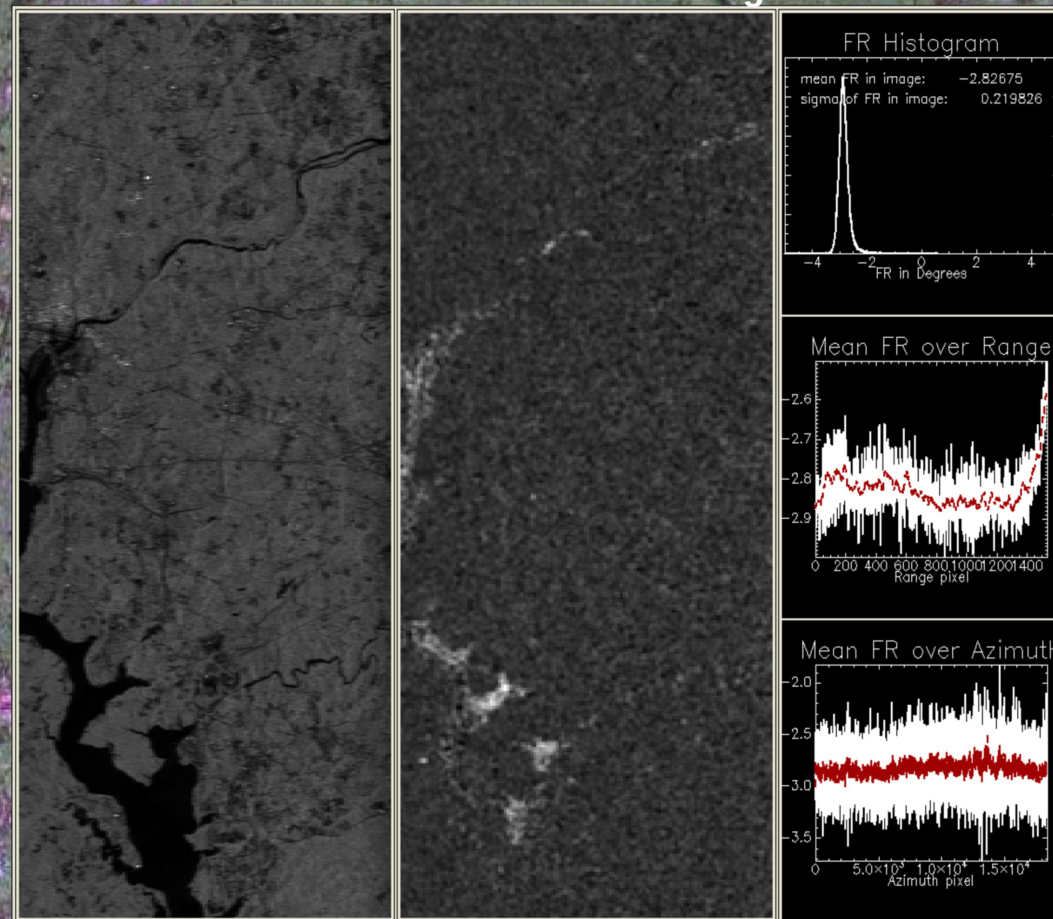

FR Correction

- Calibration and correction of FR by model inversion:

$$\begin{bmatrix} \tilde{S}_{hh} & \tilde{S}_{vh} \\ \tilde{S}_{hv} & \tilde{S}_{vv} \end{bmatrix} = \begin{bmatrix} \cos\Omega & -\sin\Omega \\ \sin\Omega & \cos\Omega \end{bmatrix} \cdot \begin{bmatrix} M_{hh} & M_{vh} \\ M_{hv} & M_{vv} \end{bmatrix} \cdot \begin{bmatrix} \cos\Omega & -\sin\Omega \\ \sin\Omega & \cos\Omega \end{bmatrix}$$

- FR Correction software allows both the correction for constant Ω and the correction for spatially varying Ω
- Example:

HV – VH before correction

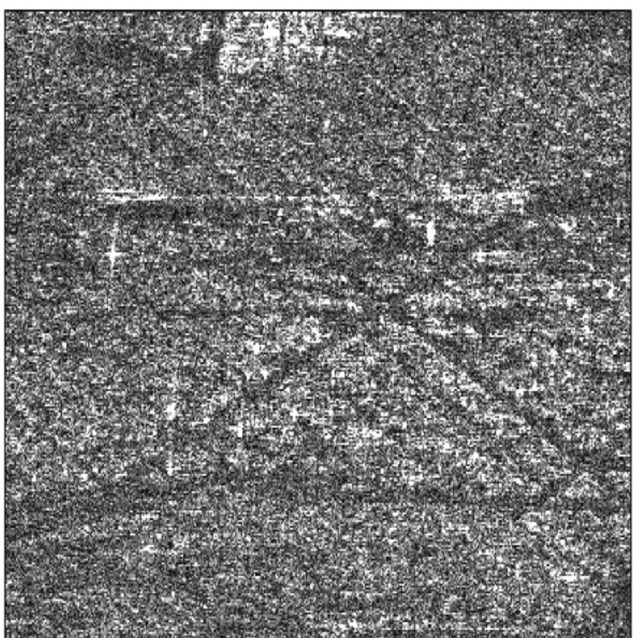

HV – VH after correction

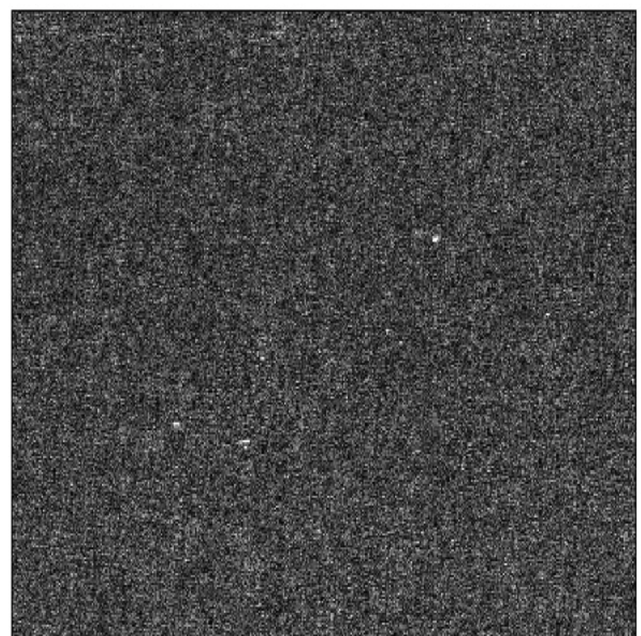

Data waiting to be explored:

- PALSAR L-Band
  - Greenland (including POLINSAR)
  - Alaska
  - Amazon
- TerraSAR-X
- Envisat
- Airborne

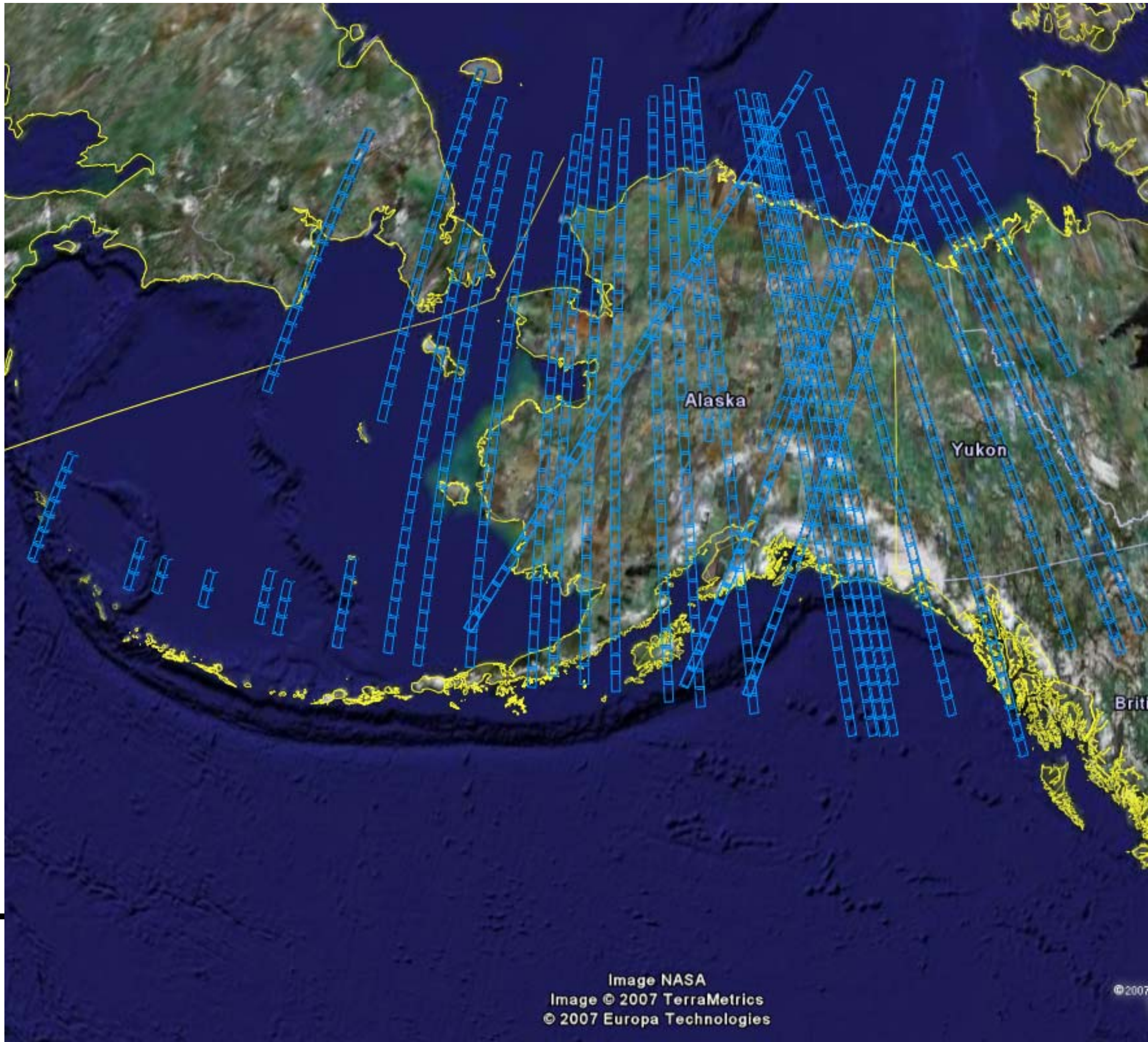

Sensors

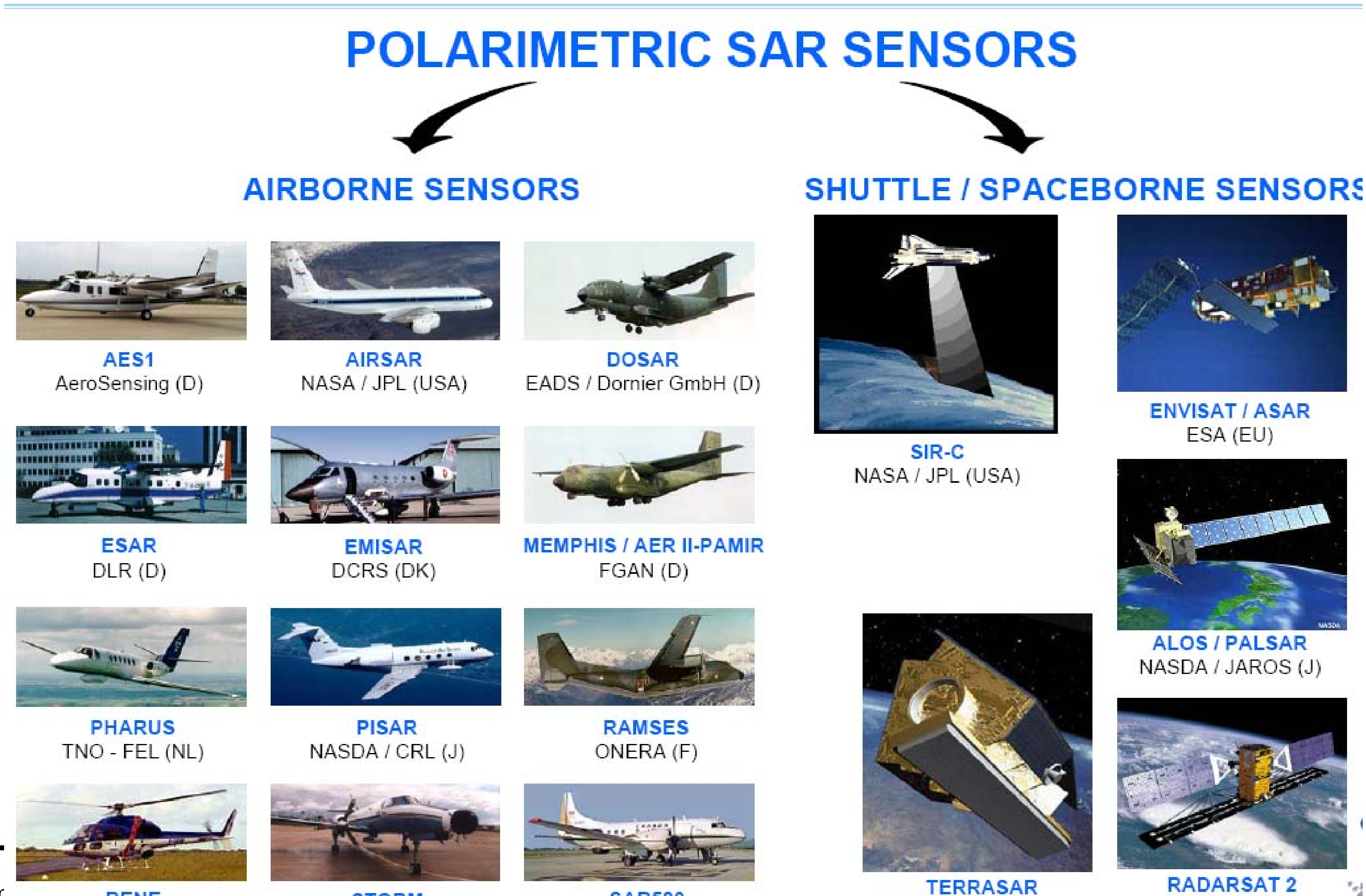

Image from Eric Pottier, Radar polarimetry basic theory